

Chapter 8

Measurement of Structural Damping

8.1. Introduction

Material damping and structural damping concerning the sample as a whole cannot be dissociated from the dynamic responses of the sample. The question we try to present in this chapter is how to relate these two coefficients with the objective of evaluating material damping without recourse to a solution of the viscoelastic inverse problem?

In some cases, it is possible to find an explicit relationship between the material damping coefficient and the sample damping coefficient, particularly around resonance frequency.

Complex modulus is, in many cases, related to sample structure by simple relationships at and around resonance frequencies of the transfer function¹. In these regions, the transfer function can be simplified and the interest of the method presented here is that it requires less sophisticated methods, simple apparatus and computer codes. As the measurements and interpretation are restricted to dynamic response around resonance frequencies, the results obtained are not as complete as those obtained by solving the inverse problem directly using the whole complex transfer function using all the information contained in real and imaginary parts or in polar representations (gain and phase).

Chapter written by Jean Tuong VINH

¹ Defined as the ratio of output signal over the input signal.

The method presented in this chapter is applicable only for low damping materials ($\tan \delta \approx 10^{-2}$). It constitutes a particular case in the solution of the inverse problem.

8.1.1. *Material damping*

There are two methods to evaluate damping coefficients of materials in viscoelasticity. The first is derived from a long (or short) transient method which allows creep (or relaxation) curves versus time to be obtained. Appropriate formulae or Fourier transforms are then used to obtain complex viscoelastic moduli (or compliances) versus frequency; see [FER 70], [VIN 67].

The second method is directly applied in the frequency domain. By vibrations of rods (or other structures), the damping capacity of a material is deduced using the dynamic responses with one or many resonances. Using this method, one obtains a reduced number of damping coefficients at the eigenfrequencies of the sample.²

The damping coefficient of the structure is not the material damping coefficient which is intrinsically attached to the viscoelastic material itself. This problem deserves some preliminary restatement.

If the sample is considered a spring dashpot and mass in parallel, the mechanical structure is considered a single degree of freedom system (SDOF) with mass, damper and stiffness. In this case, the experimenter does not use the partial derivative equation of motion but a simple equation of motion, in which the time variable is the only variable.

This hypothesis is *a priori* attractive in application and is often used in rheology. However, the range of frequency must be limited to lower frequencies, and often below the first resonance frequency.

8.1.2. *Damping coefficient of material evaluated in harmonic regime*

The second class of methods uses vibrations of a sample over a large frequency range.

Rod vibrations are governed by partial differential equations of motions with one (or more) space variables and a time variable.

² This method is applicable in a case where the expression of the transfer function versus the eigenvalues lends itself to an expansion of the characteristic functions into series.

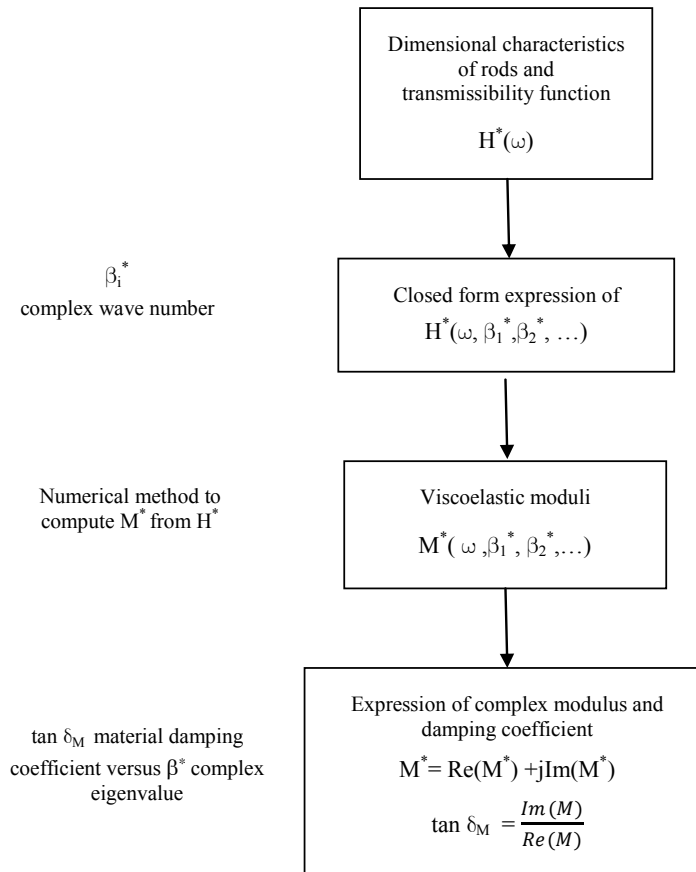


Figure 8.1. Damping capacity of material is evaluated via the structural damping. Successive steps of calculations

The stationary waves in bounded media give rise to eigenvalues β_i which depend on boundary conditions imposed on the sample.

The elastic modulus is deduced via the closed form expression of the transfer function. The correspondence principle permits a complex transfer function versus complex eigenvalues to be obtained.

Consequently, there are two steps in the calculation of material damping coefficients (Figure 8.1). We take the closed form expression of the transmissibility function into account, including eigenvalue β_i^* as parameters.

In the domain of modal analysis applied to mechanical structures, all kinds of vibrations (impact, white noise, sinusoidal, etc.) are used. Tremendous progress has been obtained, not only in the equipment to produce a great variety of excitations but also in the analyzers to obtain, by signal processing and fast Fourier transforms, a variety of functions with one, two or more input signals. In the field of signal post-processing, a great number of computer codes are available in structural dynamics.

Aside from the complex transfer function (Figure 8.1) used to solve the inverse problem, we will try to examine the possibility of simpler methods, offered by recent progress in the domain of structural dynamics.

The complex transfer functions (see [CHE 10]) corresponding to various kinds of rod vibrations, in the perspective to obtain material damping, takes into account the possible sets of boundary conditions adopted by the experimenters.

The first part of this chapter is devoted to an overview of available methods to obtain structural damping. In the second part we will present some simple methods to evaluate material damping coefficients.

8.2. Overview of various methods used to evaluate damping ratios in structural dynamics

8.2.1. Damping ratio Z deduced from one isolated resonance curve

Let us recall briefly the definition of Z for a single degree of freedom system (SDOF):

The equation of motion of the mechanical system is

$$m \frac{d^2 y}{dt^2} + c \frac{dy}{dt} + k y = f(t) \quad [8.1]$$

in which m , c and k designate mass, damping, and stiffness, respectively, and $f(t)$ is applied force. In a harmonic regime, ω being circular frequency:

$$f(t) = F_0 \sin \omega t \quad [8.2]$$

The transfer function H is defined as:

$$H(\omega) = \frac{1}{[-\omega^2 m + k + jc\omega]} = \frac{Y}{F} \quad [8.3a]$$

with Y and F being the Fourier transforms of $y(t)$ and $f(t)$ respectively.

The absolute value of $H(\omega)$ is:

$$|H(\omega)| = \frac{1}{m\left[\left(\frac{k}{m} - \omega^2\right)^2 + \left(\frac{c\omega}{m}\right)^2\right]^{1/2}} \quad [8.3b]$$

k/m is recognized as the square of undamped natural circular frequency of the system:

$$\frac{k}{m} = \omega_0^2 \quad [8.4]$$

$$|H(\omega)| = \frac{1}{m\left[(\omega_0^2 - \omega^2)^2 + c^2 \frac{\omega^2}{m^2}\right]^{1/2}} \quad [8.5]$$

The damping ratio Z is defined as:

$$Z = \frac{c}{2m\omega_0} \quad [8.6]$$

Bringing [8.6] into [8.3] and setting m as a factor in the denominator:

$$[H(\omega)]^2 = \frac{1}{m\left[-\omega^2 + \omega_0^2 + j2Z\omega\omega_0\right]} \quad [8.7]$$

This is the canonical form of a second order equation in harmonic regime of a SDOF mechanical system.

Before presenting various methods for the calculation of Z , let us remark that Z is a dimensionless coefficient and the ratio c/m has the dimension of a circular frequency.

8.2.2. The half power bandwidth

The half power bandwidth is extensively used in electrical engineering to characterize electrical elements as an inductance, L , for example, with its own resistance R . An apparatus used in this field, called a Qmeter, permits the quality coefficient to be evaluated:

$$Q = \frac{R}{L\omega}$$

The coefficient Z is equal to half of the inverse of Q :

$$\frac{1}{2Q} = Z$$

Electrical engineers and electronics experts know that the aforementioned definitions are only valid if the quality coefficient Q is at least of the order of 100.

At resonance frequency ω_r , the transfer function H^* reaches its maximum value $H^*(\omega_r)$ which is taken as a reference value. By varying the angular frequency in such a manner that equation [8.8] is satisfied (with the corresponding power³ being the half value of this power at resonance frequency), we obtain two frequencies which delimit the bandwidth:

$$\omega_{min} \leq \omega \leq \omega_{max}$$

$$\left| H(\omega = (\omega_{min} \text{ or } \omega_{max})) \right|^2 = \frac{1}{2} \left| H(\omega_r) \right|^2 \quad [8.8]$$

The bandwidth corresponds to the relative amplitude of $1/\sqrt{2} = 0.707$ with respect to the value of $\left| H(\omega) \right|$ at resonance frequency ω_r .

8.2.2.1. Amplitude of transfer function at resonance frequency ω_r

Equation [8.7] is rewritten as:

$$\left| H(\omega) \right| = \frac{1}{m \left| (-\omega^2 + \omega_0^2) + j2Z\omega\omega_0 \right|} = \frac{1}{mD}$$

with

$$D = [(\omega_0^2 - \omega^2)^2 + 4Z^2\omega_0^2\omega^2]^{1/2} \quad [8.9]$$

The derivative of [8.9] equalized to zero gives:

$$\omega_{res}^2 = \omega_0^2 (1 - 2Z^2) \quad [8.10]$$

³ The power, defined in the sense of signal processing, corresponds to the square of transfer function $\left| H(\omega) \right|^2$.

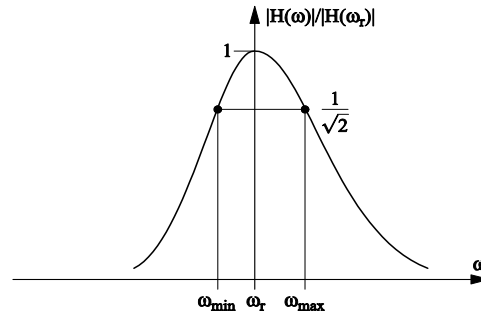


Figure 8.2. The resonance curve of an SDOF mechanical system $|H(\omega)|$. The bandwidth corresponds to the relative amplitude of $1/\sqrt{2} = 0.707$ with respect to the value of $|H(\omega_r)|$ at resonance frequency ω_r .

8.2.2.2. Frequency bandwidth

The value of D_{res}^2 at resonance frequency $\omega = \omega_{\text{res}}$ is obtained by the time derivative of [8.9]:

$$D^2 = D_{\text{res}}^2 = [\omega_0^2 - \omega^2 (1 - 2Z^2)]^2 + 4Z^2 \omega_0^4 (1 - 2Z^2)$$

$$D_{\text{res}}^2 = 4Z^2 \omega_0^4 (1 - Z^2) \quad [8.11]$$

The amplitude of $|H(\omega)|$ at the limits of the bandwidth corresponds to two times D_{res}^2 :

$$D_{\text{BW}}^2 = (\omega_0^2 - \omega^2)^2 + 4Z^2 \omega_0^2 \omega^2 = 8Z^2 \omega_0^4 (1 - Z^2) \quad [8.12]$$

Solving equation [8.12], we obtain:

$$\omega^2 = \omega_0^2 (1 - 2Z^2) \pm 2Z \omega_0^2 (1 - Z^2)^{1/2}$$

The difference between the two roots ω_{max}^2 and ω_{min}^2 is:

$$\omega_{\text{max}}^2 - \omega_{\text{min}}^2 = 4Z \omega_0^2 (1 - Z^2)^{1/2} \quad \text{or}$$

$$\omega_{\text{max}} - \omega_{\text{min}} = 4Z \omega_0^2 (1 - Z^2)^{1/2} / (\omega_{\text{max}} + \omega_{\text{min}}) \quad [8.13]$$

8.2.2.3. *First approximation for the damping ratio Z*

$$\omega_{\max} + \omega_{\min} \cong 2\omega_0(1-2Z^2)^{1/2} \quad [8.14]$$

The relative bandwidth is used to determine Z:

$$(\omega_{\max} - \omega_{\min}) / [\omega_0(1-2Z^2)^{1/2}] \cong 2Z(1+Z^2/2) \quad [8.15]$$

The applicability of this equation depends on the value of Z itself. In practice:

$$Z \leq 5 \cdot 10^{-2} \quad [8.16]$$

For damping coefficients exceeding this value, higher approximation formulae are necessary.

8.2.3. *Polar representation of transfer function: Nyquist-Argand's plot*

Polar coordinates are widely used for an SDOF system. But the majority of publications in the technical literature are devoted to systems with low damping whose value is indicated above, in [8.16].

This section concerns medium and high values of the damping ratio:⁴

$$5 \cdot 10^{-2} \leq Z \leq 1 \text{ to } 5 \quad [8.17]$$

Presented below is the currently accepted position in structural dynamics (see inequality [8.16]) so that the resonance frequency ω_{res} is assimilated to ω_0 (equation [8.10]).

The absolute value of $H(\omega)$ is rewritten as⁵:

$$|H(\omega)| = [m\omega_0^2 \sqrt{(1-\beta^2)^2 + 2jZ\beta}]^{-1/2} \quad [8.18]$$

with $\beta = \frac{\omega}{\omega_0}$, ω_0 , and undamped natural frequency: $\omega_0^2 = \frac{k}{m}$.

4 Special composites, elastomers and solid propellants have high damping capacity, say, $\tan \delta$ which can exceed 3.

5 β used here is the notation adopted in structural dynamics and is not the eigenvalue commonly used for the vibration of rods.

The phase angle is:

$$\phi = - \text{Arc tan} \frac{2Z\beta}{1-\beta^2} \quad [8.19]$$

8.2.4. *Applicability of the circle fit technique to the evaluation of damping ratio*

The circle fit technique is extensively used in modal analysis. In this section, we focus the reader's attention on the limit of this method when it is applied to the measurement of material damping. We must be aware of its shortcomings.

8.2.4.1. *Circle representation*

In Argand's plot of $H(\omega)$, the imaginary part $\text{Im}[H(\omega)]$ is represented versus the real part $\text{Re}[H(\omega)]$. The adopted hypothesis is that resonance occurs when the real part of the denominator equals zero:

$$\beta = \frac{\omega}{\omega_0} = 1$$

The transfer function becomes purely imaginary. This hypothesis is valid for low damping $Z \leq 10^{-2}$. In this case, the natural frequency is assimilated to resonance frequency.

In Figure 8.2, Argand's plot corresponds to high structural damping which is adopted as a parameter:

$$Z \in (0.1, 0.2, 0.3, 0.4, 0.5)$$

8.2.4.2. *Resonance frequency and relative bandwidth*

Equation [8.10] gives the resonance frequency

$$\omega_{\text{res}} = \omega_0 (1-2Z^2)^{1/2}$$

The relative bandwidth (RBW) is given by equation [8.14], with limited expansion of $(1-Z^2)^{1/2}$ and $(1-2Z^2)^{1/2}$:

$$\text{RBW} = (\omega_{\text{max}} - \omega_{\text{min}}) / \omega_{\text{res}} \cong 2Z(1+Z^2/2) \quad [8.20]$$

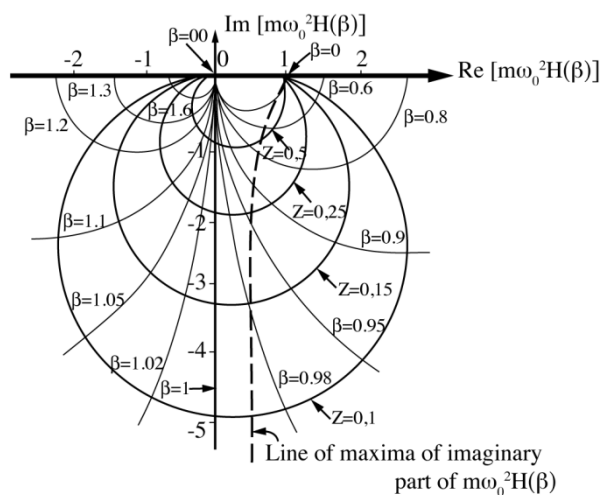


Figure 8.3. Polar Argand-Nyquist plot of dimensionless response of an SDOF system; see equation [8.21]

In Figure 8.3, $H^*(\omega)$ is represented in dimensionless form:

$$H^*(\omega) = \frac{1}{m\omega^2} D^{-1} \Phi \quad [8.21]$$

with $D = [(1-\beta^2)^2 + 4Z^2\beta^2]^{1/2}$ and $\Phi = \tan^{-1} [-2Z\beta / (1-\beta^2)]$, $\beta = \omega/\omega_0$.

The dimensionless polar coordinate is $\rho / \rho_0 = D^{-1/2}$, $\rho_0 = m\omega^2$.

For $Z = 0.1$, the angle Φ at resonance frequency is $-84^\circ 23'$

For $Z=0.5$ the angle $\Phi_{\text{resonance}} = -54^\circ 13'$

Figure 8.4 shows the frequency responses (in absolute values) which becomes more and more dissymmetric with respect to resonance frequency for high damping. The approximation in [8.20] becomes problematic, taking into account the adopted value of $(\omega_{\min} + \omega_{\max}) = 2\omega_0$.

In polar Argand's representation the circle radius becomes increasingly small with increasing damping coefficient Z . Briefly we will list the shortcomings of polar Argand's method:

- For high structural damping, accuracy of the method is poor.
- Relationship between material damping and structural damping depends on boundary conditions imposed on the sample and also on the type of vibration and the adopted hypothesis concerning displacement field.
- In the case where a closed form relationship between these two aforementioned damping coefficients, characteristic functions (which are a combination of trigonometric functions and hyperbolic functions) requires expansion into series and often simple relationships are obtained only in the case of low material damping $\tan \delta$
- High damping material gives rise to a large bandwidth, as shown in Figure 8.4, in which constancy of material damping versus frequency is not ensured. Utilization of this method becomes problematic.
- In many circumstances, complete polar representation of transfer function, Figure 8.5, includes many loops which are closed and the accuracy to obtain circles is poor. This is due to the truncated information obtained for each circle.

8.3. Measurement of structural damping coefficient by multimodal analysis

Our interest is focused on measurement of viscoelastic characteristics of materials over a large range of frequencies including a large number of vibration modes.

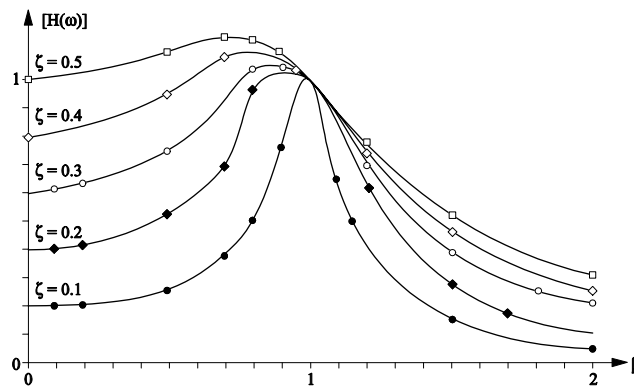


Figure 8.4. Frequency response $|H(\omega)|$ versus dimensionless frequency $\beta = \omega/\omega_0$, and ω_0 undamped natural frequency. $H(\omega)$ is represented by the dimensionless coordinate $H_r(\omega) = H(\omega)/H(\omega = \omega_0)$. The “phase resonance” with $\text{Re}(H(\omega_0)) = 0$. The amplitude resonance depends on damping ratio $Z = \omega_0(1 - 2Z^2)^{1/2}$

In the dynamics of structures, over the last three decades, a great deal of research has been devoted to the problem of modal analysis extraction techniques which merit the attention of those experimenting in linear viscoelasticity. The technical literature is very prolific in this respect. We have tried, in this chapter, to mention the principal methods which are widely used in structural dynamics. Our perspective is oriented towards possibilities of application to material characterization.

8.3.1. Overview of modal parameter extraction methods

There are two types of method: frequency domain methods and time domain methods.

8.3.1.1. Frequency domain methods and the circle fit technique

Systems responses are obtained by various excitations: sinus, random and impact. The complex transfer function is evaluated in gain and phase or in real and imaginary parts.

Modal extraction is based on Klosterman's work [KLO 71]. Argand-Nyquist's graphical representation is used; see Figure 8.5. The graphical representation shows a certain number of loops which are more or less partly opened. The problem is to fit a circle on each loop and the characteristics of the circle give rise to the frequency dependent damping coefficient Z and the eigenvalues of the modes. The circle fit technique gives rise to a least square error algorithm, which optimizes modal parameters [SDR 80]. This method is widely used in industry but is applicable to damping ratio measurement only in the case where $Z \leq 5 \cdot 10^{-2}$. The same remarks represented in the preceding section are applicable here.

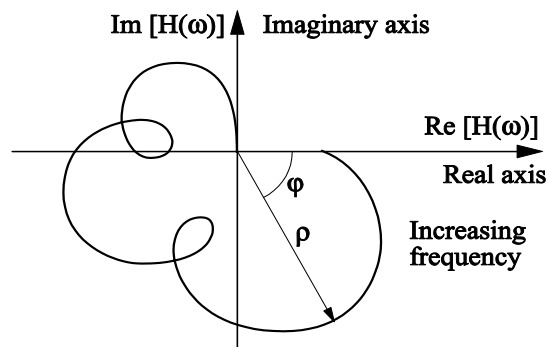


Figure 8.5. Nyquist's plot of the transfer function; ω being the parameter

8.3.1.2. Frequency domain method using rational fraction polynomials

The transfer function is expressed as a quotient of two polynomials as:

$$H(\omega) = \frac{\sum_{k=0}^{2N-1} a_k(j\omega)^k}{\sum_{k=0}^{2N-1} b_k(j\omega)^k} \quad [8.22]$$

The error function e_m is defined as the difference between the analytical transfer function defined in [8.22] and the experimental transfer function $H_e(\omega)$:

$$e_m = \frac{\sum_{k=0}^{2N-1} a_k(j\omega)^k}{\sum_{k=0}^{2N-1} b_k(j\omega)^k} - H_e(\omega_m) \quad [8.23]$$

The gradient method is used to minimize the error vector, as one has to deal with ill-conditioned matrices.

After obtaining coefficients of the rational fraction, modal parameters are evaluated. The roots of the denominator root or poles contain the values of the material frequency and damping ratio.

8.3.1.3. Time domain method using Prony's complex exponential series

A multi degree of freedom system (MDOF) is defined as a sum of N transfer functions of single degree of freedom systems (SDOFs). The transfer function is represented as:

$$H_{ik}(\omega) = \frac{Y_i(\omega)}{F_k(\omega)} = \sum_{r=1}^N \frac{A_{ik}^r}{\omega_r Z_r + j(\omega - \omega_r \sqrt{1 - Z_r^2})} + \frac{A_{ik}^{*r}}{\omega_r Z_r + j(\omega + \omega_r \sqrt{1 - Z_r^2})} \quad [8.24]$$

The star superscript designates a conjugate quantity. Another way of writing [8.24] is to collect the complex conjugate poles in a unique set of a system of 2N degrees of freedom:

$$H_{ik}(\omega) = \sum_{r=1}^{2N} \frac{A_{jk}^r}{\omega_r + Z_r + j(\omega - \omega_r)} \quad [8.25]$$

$$\left. \begin{aligned} \omega' &= \omega_r \sqrt{1 - Z_r^2} \\ \omega'_{r+N} &= -\omega'_r \\ A_{jk}^{r+N} &= A_{jk}^* \end{aligned} \right\} \quad [8.26]$$

The complex exponential method works with the impulse response of the system obtained by inverse Fourier transform of the transfer function [8.22]:

$$h_{jk}(t) = \sum_{r=1}^{2N} A_{jk}^r e^{s_r t} \quad [8.27]$$

An example of impulse response function is represented in Figure 8.6. The total time duration can be evaluated by the impulse response function. It can be divided into intervals with $\Delta t =$ value of the time increment.

$$t_0=0, t_1 = \Delta t, t_2= 2\Delta t, \dots, t_L= L\Delta t \quad [8.28]$$

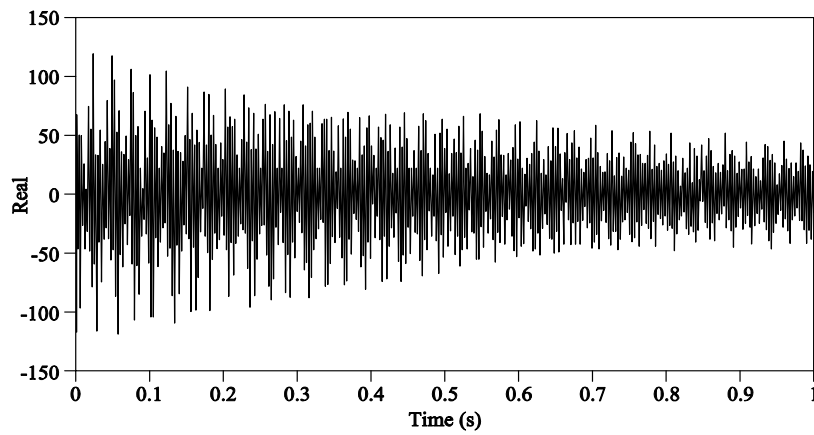


Figure 8.6. Impulse response function of a multimodal system

Let us adopt the following notations:

$$\left. \begin{aligned} h_0 &= h(0) = \sum_{r=1}^{2N} A_r' \\ h_1 &= h(\Delta t) = \sum_{r=1}^{2N} A_r' e^{s_r \Delta t} \\ \dots \dots \dots \\ h_L &= h(L\Delta t) = \sum_{r=1}^{2N} A_r' e^{s_r L\Delta t} \end{aligned} \right\} \quad [8.29]$$

The problem is to evaluate all the components in [8.29], the first member h_1 being known, the factors in the second member: the coefficients A_r' and the exponentials are evaluated by an algorithm using a polynomial of order L , with a real coefficient β called an autoregressive coefficient [VOL 82].

When the exponential terms have been evaluated, the exponent $s_r \Delta t$ is obtained. The circular natural frequency and damping ratio of r mode are calculated:

$$\omega_r = s_r \quad ; \quad Z_r = \frac{1}{1 + \left[\frac{Im(R_r)}{Re(R_r)} \right]^2} \quad \text{with } R_r = s_r \Delta t \quad [8.30]$$

8.4. The Hilbert envelope time domain method

This method permits the envelope of the impulse response to be extracted from exponentially decreasing oscillations. The Hilbert transform of time is extensively used in digital signal processing. It is described by the following equation, where the star represents a linear convolution, and \mathfrak{H} and \mathfrak{F} are the Hilbert transform and Fourier transform, respectively:

$$\mathfrak{H}[x(t)] = X_H(t) = -\frac{1}{\pi t} * x(t) = \mathfrak{F}^{-1}[\mathfrak{F}(j\omega) \cdot X(j\omega)] \quad [8.31]$$

The Fourier transform of $-1/\pi t$ is $j(\text{sign } \omega)$, which is $+j$ for positive ω and $-j$ for negative ω . Consider the Hilbert transform of time, in which an even function is odd and the Hilbert transform of an odd function is even.

The practical interest of the Hilbert transform of time is to transform negative sine into cosine and negative cosine into a sine component.

The original signal and its Hilbert transform are combined to form an analytic signal:

$$x(t) = x(t) - j x_H(t) \quad [8.32]$$

8.4.1. The practical interest of the Hilbert transform of time

The magnitude of the analytical signal is the envelope of the original time signal. The envelope is plotted on a decibel scale, so that the graph is a line.

For an SDOF system:

$$x(t) = A e^{-Zt\omega_0} [\sin(\omega_0 t \sqrt{1 - Z^2})] \quad [8.33]$$

Its Hilbert transform of time is :

$$X_n(t) = A e^{-Z\omega_0 t} [\cos(\omega_0 t \sqrt{1-Z^2})] \quad [8.34]$$

The analytical signal is:

$$x_A(t) = A e^{-Z\omega_0 t} [\sin(\omega_0 t \sqrt{1-Z^2}) + \cos(\omega_0 t \sqrt{1-Z^2})] \quad [8.35]$$

The magnitude of the analytical signal is:

$$\begin{aligned} |x_A(t)| &= A e^{-Zt\omega_0} [\sin^2 \omega_0 t \sqrt{1-Z^2} + \cos^2 \omega_0 t \sqrt{1-Z^2}] \\ |x_A(t)| &= A e^{-Zt\omega_0} \end{aligned} \quad [8.36]$$

Consequently the method improves the calculation accuracy for Z with the condition that each mode must be isolated from the other in a frequency domain. If the frequency interval chosen is too large, the proximity of other modes has an influence on the logarithmic decrement with eventually parasitic oscillations. Figure 8.7 gives an example of the Hilbert envelope method, after Iglesias [IGL 00].

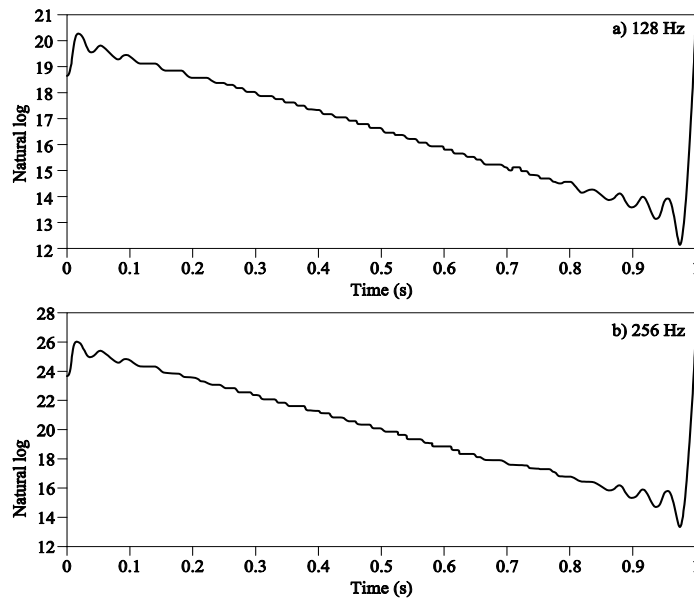


Figure 8.7. Hilbert transform of time applied to an impulse response function. Each mode is separated and treated in the time domain. A natural logarithm is applied to the envelope of the impulse response. Oscillations on the curve are due to an isolating window, after Iglesias [IGL 00]

8.5. Detection of hidden non-linearities

In Chapter 7, the Hilbert transform for frequency was presented. Its interest, for damping ratio estimates, resides in the fact that it does not require any *a priori* non-linearity models.

The non-causal part of the frequency response can be detected by evaluating the positive and negative parts of the Hilbert transform which permit the experimenter to evaluate the degree of pollution of the frequency response by the following possible causes:

- a) non-linearities from the transducers;
- b) non-linearities due to the high level of force applied to the sample.

In a case where non-linear behavior of the viscoelastic sample is important, the problem must be examined in another framework, e.g. looking at the non-linear behavior of the material using the Volterra functional series.

8.6. How to relate material damping to structural damping?

So far, we have presented the damping ratio of a sample (considered to be a mechanical structure) being evaluated. But how do we relate material damping to structural damping? In a previous publication [CHE 10] we have addressed this problem directly, considering material damping versus frequency. In this chapter, one parameter of the material (the damping coefficient) is directly deduced from structural damping, and an estimation of the complex modulus at and around resonance frequency is made.

Our proposed process to solve this is as follows:

- a) from the transfer function expressed in a closed form expression, an attempt is made to relate material damping to sample (structural) damping for each eigenmodes;
- b) if possible, for low material damping ($\tan \delta \approx 10^{-2}$), a limited expansion of hyperbolic and trigonometric functions used in the transfer function is effected around the resonance frequency;
- c) evaluation of $\tan \delta$ is effected via the structural damping ratio Z .

8.6.1. Example: flexural vibration of a clamped-free Bernoulli-Euler's rod

The transmissibility of the rod is:

$$H(\omega) = \frac{\cos \beta^* + \cosh \beta^*}{1 + \cos \beta^* \cdot \cosh \beta^*} \quad [8.37]$$

The force excitation is applied at the clamping end, whilst the other end is free. In the case of a low damping material ($\tan \delta \approx 10^{-2}$) the eigenvalues are, in practice, those obtained in an elastic regime. This corresponds to the poles of [8.37]:

$$\beta_{01} = 1.875104 ; \beta_{02} = 4.694091 ; \beta_{03} = 7.855 ; \beta_{04} = 10.996 \quad [8.38]$$

$$\beta_{0n} \cong \frac{(2n-1)\pi}{2} \quad \text{with } n > 4$$

Bernoulli's equation permits the relationship between a complex wave number and a complex Young's modulus⁶ to be obtained:

$$E^* = \frac{\omega^2 L^4 \rho S}{\beta^{*4} I} \quad [8.39]$$

where L is the rod length, S the cross-section area, ρ density, ω circular frequency, I cross-section inertia with respect to the neutral line. The star designates a complex quantity.

8.6.1.1. Sharpness of the resonance curve

In the case of low material damping, the imaginary part of complex β^* varies very slowly and it is reasonable to hypothesize that this imaginary part is practically constant; and we write:

$$\beta_k^*(\omega) \cong \beta_{0k} (1 - j \tan \delta_E) \quad [8.40]$$

β_{0k} is the wave number at resonance for the k^{th} mode (equation [8.38]).

⁶ Imaginary part of Young's modulus is positive while the imaginary part of β^* is negative after [8.39].

Around the resonance frequency the logarithmic variation of ω is:

$$\Delta\omega / \omega = 2\Delta\beta / \beta \cong 2\Delta\beta_1 / \beta_1 \quad [8.41]$$

The sharpness of the resonance curve is:

$$\beta(\omega) = \beta_1 - j\beta_2 \cong (\beta_{01} + \Delta\beta_1) - j\beta_2 \quad [8.42]$$

With this approximation, we are able to express the transfer function as an amplification coefficient α :

$$H(\omega) = \alpha = \frac{\cos\beta_1 + \cosh\beta_1 - j\beta_2(\sinh\beta_1 - \sin\beta_1)}{1 + \cos\beta_1 \sinh\beta_1 - j\beta_2(\cos\beta_1 \sinh\beta_1 - \sin\beta_1 \cosh\beta_1)} \quad [8.43]$$

For a weak value of β_2^7 , $\sinh \beta_2$ and $\sin \beta_2$ are assimilated to β_2 . [8.43] takes into account the variation $\Delta\beta_1$ in [8.41] :

$$H(\omega) = \frac{N}{D}$$

where the numerator N and denominator D take the following expressions:

$$\begin{aligned} N &= \cos\beta_0 + \cosh\beta_0 + \Delta\beta_1(\sinh\beta_0 - \sin\beta_0) - j\beta_2[(\sinh\beta_0 - \sin\beta_0) + (\cosh\beta_0 - \cos\beta_0)] \\ D &= (\Delta\beta_1 - j\beta_2)(\cos\beta_0 \sinh\beta_0 - \sin\beta_0 \cosh\beta_0) + 2j\beta_2\Delta\beta_1\sin\beta_0\sinh\beta_0 \end{aligned} \quad [8.44]$$

For convenience, in [8.44] the subscript 0 concerns a value of β_{0n} at resonance frequency. To specify the order of the wave number, as in [8.38], a second number n is written after 0 in the subscript.

8.6.1.2. Amplification factor at resonance frequency

[8.38] gives the value of wave number at resonance frequency. Bringing one of these values for β_0N into [8.44] and equalizing $\Delta\beta_1 = 0$, we obtain (for example) the lowest resonance frequency corresponding to β_{01} in [8.38]:

$$|H(\omega)| = |\alpha_{1\text{resonance}}| = \left| \frac{3.0375 - j2.2963\beta_2}{j\beta_2 \cdot 4.2275} \right| \quad [8.45]$$

⁷ This assumption is valid if the damping coefficient $\tan \delta_E$ is weak.

The first part of [8.45] being obtained by experiment, this equation allows β_2 to be obtained:

$$|\alpha_{1\text{resonance}}| \cong 0.51627\left(\frac{1}{\beta_2^2} + 0.5715\right) \quad [8.46]$$

The damping coefficient is then deduced:

$$\tan \delta_E = \frac{\text{Im}(E^*)}{\text{Re}(E^*)} \cong \frac{1.5328}{\alpha_{1\text{resonance}} \left(1 - \frac{0.1472}{\alpha_{1\text{res}}^2}\right)} \quad [8.47]$$

8.6.1.3. Material damping versus bandwidth

With respect to the amplitude of the transfer function α_{res} at resonance frequency, the amplitude at the bandwidth frontier is $\alpha_{\text{res}}/\sqrt{2}$, with $2\Delta f$ being the bandwidth:

$$\tan \delta_E = |2\Delta f / f_{\text{res}}| [1 + 1.4521 \cdot 10^{-2} (2\Delta f / f) + 6.2633 (2\Delta f / f)^2]^{-1} \quad [8.48]$$

Similar equations can be obtained for higher eigenmodes, see equation [8.38]. One obtains similar equations as above with different set of coefficients.

8.6.1.4. Young's modulus

As we have to deal with material with low damping, the absolute value of the complex modulus is (taking equation [8.39]):

$$|E^*_{\text{resonance}}| \cong \frac{\omega^2 L^4 \rho S}{\beta_1^2 I}, I = bh^3/12 \quad [8.49]$$

where b is width, and h thickness.

Taking into account the validity condition in section 8.6.1.1, [8.40] the imaginary part of β^* is neglected in its absolute value:

$$|\beta^*| \cong \text{Re}[\beta^*] = \beta_1 \quad [8.50]$$

The example presented in 8.6.1 uses Bernoulli-Euler's rod. Longitudinal and torsional vibration of a viscoelastic rod can be treated in a similar manner, for various eigenmodes. For a material and sample governed by equations of a higher degree of approximation, theoretically speaking this method is applicable but at the

price of lengthy calculations using limited expansion of series for characteristic functions.

8.7. Concluding remarks

This chapter is written as a complement to the solution of the inverse problem which permits calculation, frequency by frequency, of the complex modulus. There are two interesting groups of remarks.

8.7.1. *Exploitation of resources in signal processing and computer codes in structural dynamics*

With an effort at adaptation, researchers and experimenters in material characterization, particularly in the domain of viscoelasticity, can find a variety of methods to interpret complex moduli of material, particularly when one has to deal with a large frequency range in which transfer functions are obtained. Methods to obtain eigenfrequencies and structural damping in the frequency domain and the time domain can also be achieved.

Evaluation of complex moduli and material damping is within the competence of experimenters themselves.

8.7.2. *Complementary methods to evaluate complex moduli and damping coefficients*

The methods to solve inverse problems governed by differential equations with time and space variables are presented elsewhere [CHE 10]. The solution is not restricted to a narrow low frequency range as usually adopted in experimental viscoelasticity, with the possibility of artificial expansion of the frequency (or time) range using the Williams-Landel-Ferry method.

We are convinced there are now many opportunities: there has been much progress in dynamic tests and a variety of methods for evaluating complex moduli and material damping have been developed. We have tried to show that some simplified methods are available if the hypothesis of weak damping is verified.

Readers will remember that the well-known method of half power bandwidth permits structural damping ratios to be evaluated. Relations deduced from transfer functions also allow material damping and complex moduli to be obtained in a direct manner.

The logarithmic decrement method is well known in experimental viscoelasticity. Recent progress accomplished in the analysis of structural dynamics, in the elaboration of new programs such as the Hilbert transform for time (for detecting the time response envelope with appropriate frequency filters) has contributed to seriously improve the damping ratio estimation by logarithmic decrement methods.

Multimodal methods can be extended to viscoelastic materials. Progress in digital signal processing as well as special programs devoted to the multimodal analysis of structures have suggested new tools for experimenters.

8.8. Bibliography

- [BRO 79] BROWN D.L., ALLEMANG R.J., ZIMMERMAN R., MERGEAY M.V., Parameter estimation technique for modal analysis, SAE paper, number 790221, 1979.
- [CHE 10] CHEVALIER Y., VINH J.T. (eds.), *Mechanics of Viscoelastic Materials and Wave Dispersion*, ISTE Ltd, London, John Wiley & Sons, New York, 2010.
- [FER 70] FERRY J.D., *Viscoelastic properties of polymers*, John Wiley & Sons Inc, New York, 1970.
- [ILG 00] IGLESIAS A.M., Investigating various modal analysis extraction techniques to estimate damping ratio, Master's thesis, June, Virginia Polytechnic Institute, Blackburg U.S.A., 2000.
- [KLO 71] KLOSTERMAN A., On the experimental determination use of modal representations of dynamic characteristic, PhD dissertation, University of Cincinnati, 1971.
- [MEN 97] MENDES MAIA N.M., MONTALVAO E SILVA J.M., *Theoretical and Experimental Analysis*, John Wiley & Sons Inc, New York, 1997.
- [PRO 1795] PRONY R., Essai expérimental et analytique sur les lois de la dilatabilité des fluides élastiques et sur celles de la force expansive de la vapeur de l'eau et de la vapeur de l'alcool à différentes températures, Vol.I, Cahier 2, Floréal et Prairial an III, pp. 24-76, in French, 1795.
- [RIC 82] RICHARDSON M.H., FORMENTI D.L., "Parameter estimation from frequency response measurements using ratio and fraction polynomials", *Proceedings of the International Modal Analysis Conference*, pp. 167-181, 1982.
- [SDR 89] S.D.R.C., Modal analysis user manual modal analysis approach, 1989.
- [VIN 67] VINH T., On the interrelation between harmonic and transient viscoelastic responses, *Mémorial de l'Artillerie française*, Vol III, pp. 725-776, 1967.